

Interactions of Chiral Ru(II) Complexes with Calf Thymus DNA as Studied by Circular Dichroism and Electric Dichroism Measurements

KYAW Naing, Masayuki TAKAHASHI, Masahiro TANIGUCHI, and Akihiko YAMAGISHI*

Division of Biological Sciences, Graduate School of Science, Hokkaido University, Sapporo 060

(Received February 28, 1994)

The interactions of the enantiomers of $[\text{Ru}(\text{bpy})_2(\text{phi})]\text{Cl}_2$ and $[\text{Ru}(\text{phen})_2(\text{phi})]\text{Cl}_2$ ($\text{bpy}=2,2'$ -bipyridine, $\text{phen}=1,10$ -phenanthroline, and $\text{phi}=9,10$ -phenanthrenequinone diimine) with calf thymus DNA were studied by spectroscopic titrations, circular dichroism, and electric linear dichroism methods. These complexes bound to DNA with binding constants greater than 10^4 M^{-1} . From the CD and LD spectra, the phi ligands of both complexes are concluded to be intercalated between the basepairs of DNA.

Noncovalent interactions of metal complexes with DNA have been studied with the purpose of developing a novel reagent which recognizes DNA sites to induce the cleavage of a strand.¹⁾ Noncovalent interactions are thought to take place in the following three different ways:

- (1) binding along the outside of the helix,
- (2) binding along the major and minor grooves, and
- (3) intercalation of a planar molecule or a planar aromatic ring system between basepairs.

In designing an effective cleaving metal complex, it is of vital importance to identify which of the above interaction modes is operative for the molecule concerned and which of the factors is predominant among electrostatic, hydrogen bonding, and van der Waals interactions and steric factors. For that purpose, the binding interactions between DNA and a metal chelate such as Ru, Fe, Zn, or Rh complexes have been studied.^{2–9)} $[\text{RuL}_3]^{2+}$ ($\text{L}=\text{polypyridyl}$) and its mixed ligand derivatives, for instance, are concluded to bind with DNA in two different binding interactions: (a) intercalation and (b) binding along the groove.¹⁰⁾ It has been reported that the phi ligands of both Δ - and Λ - $[\text{Ru}(\text{bpy})_2(\text{phi})]^{2+}$ ($\text{bpy}=2,2'$ -bipyridine, $\text{phi}=9,10$ -phenanthrenequinone diimine) complex show the intercalation between the base pairs of calf thymus DNA.¹¹⁾ The phi ligand of Δ - $[\text{Rh}(\text{phen})_2(\text{phi})]^{3+}$ ($\text{phen}=1,10$ -phenanthroline) complex intercalates in $[\text{d}(\text{GTCAC})_2]$.¹²⁾ The Δ - and Λ -enantiomers of $[\text{Ru}(\text{phen})_2(\text{dppz})]^{2+}$ complex, where $\text{dppz}=\text{dipyrido}[3,2-a:2',3'-c]\text{phenazine}$, intercalate between the base pairs of calf thymus DNA.¹³⁾

In this work, $[\text{Ru}(\text{bpy})_2(\text{phi})]\text{Cl}_2$ and $[\text{Ru}(\text{phen})_2(\text{phi})]\text{Cl}_2$ complexes were synthesized and resolved to opposite enantiomers. The binding interactions between an enantiomer and a duplex DNA have been studied by using spectroscopic titration, circular dichroism (CD), and electric linear dichroism (LD) methods. From spectroscopic titration results, the binding constant was calculated for each enantiomer. CD spectra showed the effects of asymmetric environments of a DNA chain on the electronic transitions of a bound complex. LD spectra point out the orientation of the ligand of a bound complex.

As a result, it has been concluded that the phi ligands

of both Δ - and Λ - $[\text{RuL}_2(\text{phi})]^{2+}$ ($\text{L}=\text{bpy}$ and phen) complexes are intercalated between the basepairs of duplex DNA.

Experimental

Ruthenium Complexes. $[\text{Ru}(\text{bpy})_2(\text{phi})]\text{Cl}_2$ and $[\text{Ru}(\text{phen})_2(\text{phi})]\text{Cl}_2$ were synthesized from $\text{RuCl}_3 \cdot x\text{H}_2\text{O}$ (Aldrich) and $\text{K}_2[\text{RuCl}_5(\text{H}_2\text{O})]$ (Johnson Matthey), respectively.^{7,14,15)} Racemic $[\text{Ru}(\text{bpy})_2(\text{phi})]\text{Cl}_2$ complex was resolved by being eluted on a CM-Sephadex column $[35 \times 1.8 \text{ cm (i.d.)}]$ with a saturated dipotassium bis(tartrato)-dianthimonate (-2) solution. The Δ -isomer was eluted first, being followed by the Λ -isomer. $\Delta\epsilon_{535}$ was calculated to be 23 and -24 for Δ - and Λ -enantiomers, respectively. For racemic $[\text{Ru}(\text{phen})_2(\text{phi})]^{2+}$, the same procedure was done and $\Delta\epsilon_{535}$ was calculated to be 16 and -16 for Δ - and Λ -enantiomers, respectively. Figure 1 shows the absolute configurations of chiral ruthenium complexes. The concentrations of $[\text{Ru}(\text{bpy})_2(\text{phi})]^{2+}$ and $[\text{Ru}(\text{phen})_2(\text{phi})]^{2+}$ were measured spectrophotometrically at 535 nm using the reported values of extinction coefficients of 48000 and 51900, respectively.⁷⁾

Double Stranded Nucleic Acids. Calf thymus DNA (Sigma) was used as purchased. The pH of a DNA solution

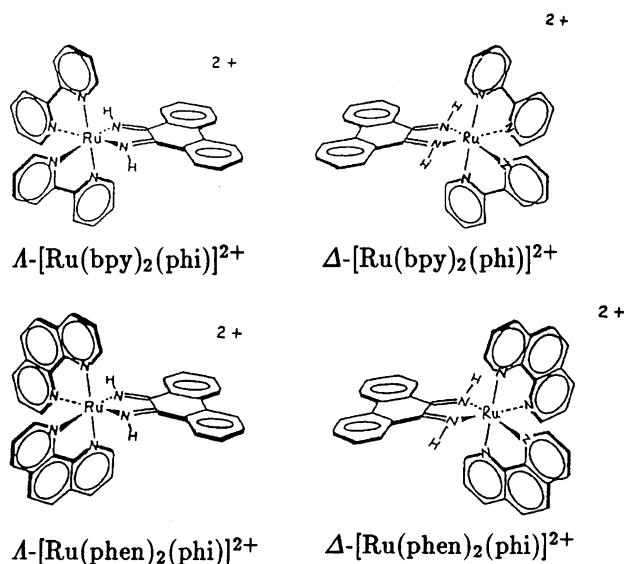


Fig. 1. Absolute configurations of chiral ruthenium complexes.

was adjusted to 7.0 with 0.001 M ($M = \text{mol dm}^{-3}$) sodium dimethyl arsinat buffer and the concentration was measured spectrophotometrically using the extinction coefficients of 6600 (260 nm).¹⁶⁾

Spectroscopic Titration. Spectroscopic titrations were done at room temperature to measure the binding strength between DNA and each enantiomer. A mixture of DNA and an enantiomer (solution A) was added gradually to a solution containing the same concentration of the enantiomer only (solution B). The details of the results are described in Results section.

CD and LD Measurements. CD spectra were recorded for a solution of a free enantiomer or a solution containing the enantiomer fully bound to a polynucleotide. LD spectra were measured with an instrument as described previously.¹⁷⁾ The field strength dependence studies of linear dichroism were done at 540 nm by changing the applied field from 540 V cm^{-1} to 5.46 kV cm^{-1} at the constant pulse width of $400 \mu\text{s}$. The wavelength dependence of dichroism was measured by applying a pulse of $5.46 \text{ kV cm}^{-1} \times 1 \text{ ms}$.

Instrumentation. Absorbance and circular dichroism measurements were done with a spectrophotometer (JASCO-Uvidec-430A) and a spectropolarimeter (JASCO-J-500A), respectively. The instrument used to measure the linear dichroism was constructed in this laboratory.¹⁷⁾

Results

Spectroscopic Titration. Two kinds of solutions were prepared for spectroscopic titration. Solution A contained a chiral metal complex and DNA. Solution B contained the same concentration of the metal complex only. In titration, solution A was added by units of 0.1 mL to 2 mL of solution B. The concentration of the chiral complex is kept constant throughout the titration. Curve 1 in Fig. 2 is the spectrum of solution B for $\Delta\text{-}[\text{Ru}(\text{phen})_2(\text{phi})]^{2+}$ ($1.85 \times 10^{-5} \text{ M}$). It has an absorption maximum at 535 nm , which is assigned to the metal-to-ligand charge-transfer (MLCT) band from a central Ru^{2+} to the phi ligand, and an absorption band around $440\text{--}470 \text{ nm}$, which is assigned to the MLCT from a central Ru^{2+} to the phen ligands.¹⁸⁾ The absorption band at 260 nm represents the local excitation of π -electrons in the phen ligands. On adding solution A containing $\Delta\text{-}[\text{Ru}(\text{phen})_2(\text{phi})]^{2+}$ ($1.85 \times 10^{-5} \text{ M}$) and DNA ($4 \times 10^{-4} \text{ M}$), the absorbance of the MLCT band at 535 nm decreases with the concomitant shift of the peak position towards a longer wavelength. The addition of solution A is done until the absorbance at 535 nm remains unchanged and attains the final spectrum as shown by curve 2 in Fig. 2. At this stage, all the chiral complex molecules are fully bound by DNA. Figure 3 shows the plot of the relative absorbance change at 535 nm (A/A_0), where A_0 and A are the absorbance of solution B and the absorbance of a mixture at each addition of solution A, respectively, against the analytical concentration of the DNA, $[\text{DNA}]_0$. A/A_0 decreases with the increase of $[\text{DNA}]_0$ until it is levelled off in the range of $[\text{DNA}]_0$ larger than $[\text{DNA}]_s$ as denoted by an arrow in the figure. The number of basepairs occupied

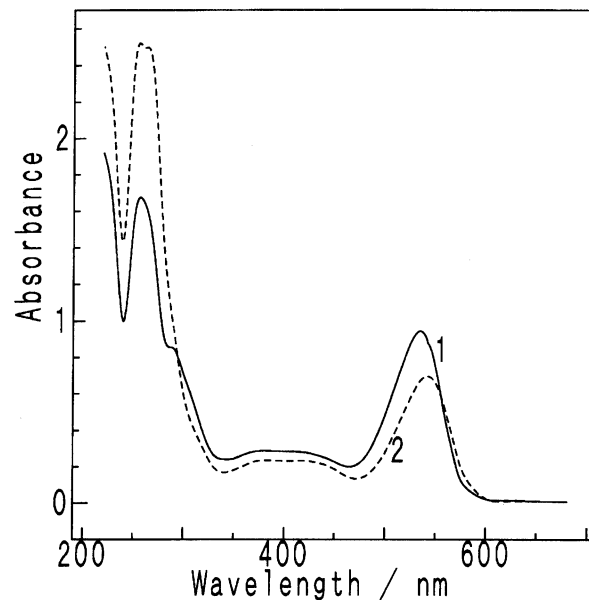


Fig. 2. Absorption spectra of (a) $\Delta\text{-}[\text{Ru}(\text{phen})_2(\text{phi})]^{2+}$ ($1.85 \times 10^{-5} \text{ M}$); (b) $\Delta\text{-}[\text{Ru}(\text{phen})_2(\text{phi})]^{2+}$ ($1.85 \times 10^{-5} \text{ M}$) and calf thymus DNA ($1.47 \times 10^{-4} \text{ M}$).

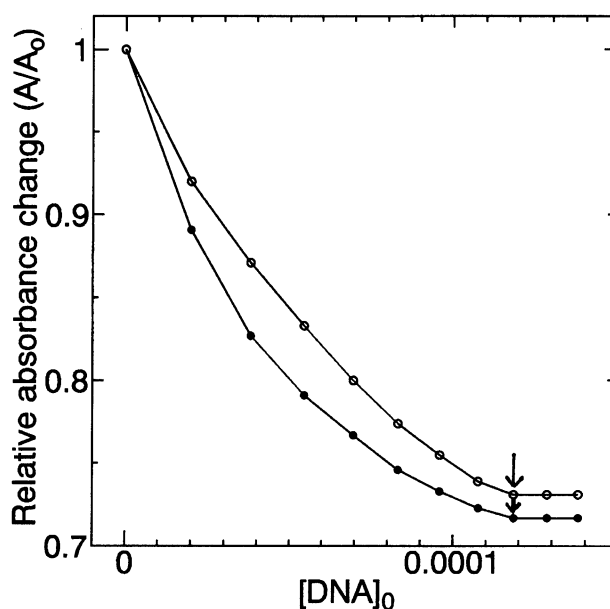


Fig. 3. Decreases of relative absorbance changes (535 nm) of $\Delta\text{-}[\text{Ru}(\text{phen})_2(\text{phi})]^{2+}$ ($1.85 \times 10^{-5} \text{ M}$) (●) and $\Lambda\text{-}[\text{Ru}(\text{phen})_2(\text{phi})]^{2+}$ ($1.83 \times 10^{-5} \text{ M}$) (○) with the addition of solution A of DNA ($4.00 \times 10^{-4} \text{ M}$). The saturated levels are indicated by arrows.

by one complex (n) is estimated approximately by the following equation:

$$n = [\text{DNA}]_s / [\text{M}], \quad (1)$$

in which $[\text{M}]$ is the concentration of the chiral metal complex. The spectral change from curve 1 to curve 2 in Fig. 2 clearly points out the binding of the metal

complex with the DNA.¹⁹⁾

The intrinsic binding constant of an enantiomer is calculated from Eq. 2,²⁰⁾

$$[\text{DNA}]/(\varepsilon_A - \varepsilon_B) = [\text{DNA}]/(\varepsilon_B - \varepsilon_F) + 1/K_B(\varepsilon_B - \varepsilon_F), \quad (2)$$

where $[\text{DNA}]$ is the equilibrium concentration of DNA and ε_A , ε_F , and ε_B correspond to absorbance/ $[\text{Ru}]$, the extinction coefficient for a free ruthenium complex (literature value) and the extinction coefficient for a bound ruthenium complex, respectively. ε_A can be calculated after each addition of solution A (0.1 ml) by equation,

$$A = \varepsilon_A \times b \times [\text{Ru}], \quad (2a)$$

where A =absorbance at 535 nm, b =cell length (1 cm), $[\text{Ru}]$ =known concentration of the chiral complex (constant concentration throughout the titration). At the end of the titration, the absorbance at 535 nm remains unchanged and ε_A becomes ε_B . In Fig. 4, $[\text{DNA}]/(\varepsilon_A - \varepsilon_B)$ is plotted against $[\text{DNA}]$ to give a straight line for each isomer. The ratio of the slope to the intercept of the straight line is equal to the binding constant, K_B .

In Table 1, the red shift (R) of the absorption peak at 535 nm (for both complexes), the average number of base pairs occupied by one chiral complex (n) and the intrinsic binding constant (K_B) are given for the enantiomers of $[\text{Ru}(\text{phen})_2(\text{phi})]^{2+}$ and $[\text{Ru}(\text{bpy})_2(\text{phi})]^{2+}$ bound to calf thymus DNA.

CD Measurements. The CD spectrum was compared between the free and fully bound enantiomers of $[\text{Ru}(\text{phen})_2(\text{phi})]^{2+}$ and $[\text{Ru}(\text{bpy})_2(\text{phi})]^{2+}$. Figure 5 shows the CD spectra for the systems of Δ - or Λ - $[\text{Ru}(\text{phen})_2(\text{phi})]^{2+}$ and calf thymus DNA. In the spec-

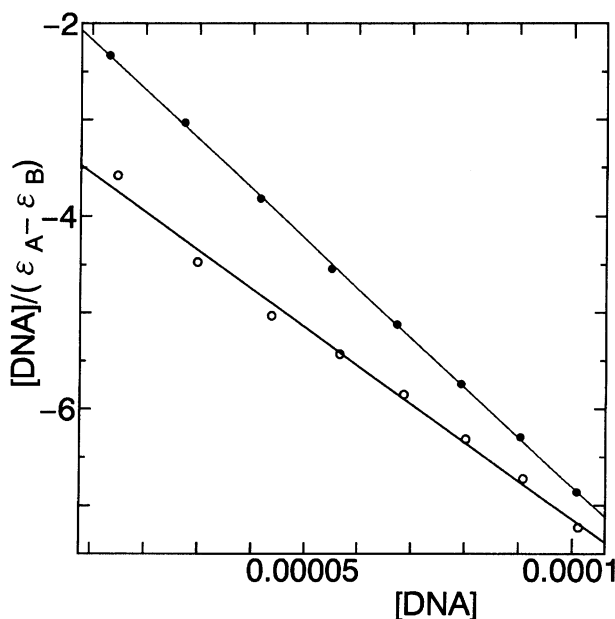


Fig. 4. Plot of $[\text{DNA}]/(\varepsilon_A - \varepsilon_B)$ vs $[\text{DNA}]$ for the systems as shown in Fig. 3.

Table 1. Binding Parameters of Chiral Ruthenium Complexes with Calf Thymus DNA

| Enantiomers | $K_B^a) \times 10^4$ | $n^b)$ | R/nm |
|---|----------------------|--------|---------------|
| Δ - $[\text{Ru}(\text{bpy})_2(\text{phi})]^{2+}$ | 1.27 | 6.1 | 8 |
| Λ - $[\text{Ru}(\text{bpy})_2(\text{phi})]^{2+}$ | 1.12 | 6.3 | 8 |
| Δ - $[\text{Ru}(\text{phen})_2(\text{phi})]^{2+}$ | 3.12 | 6.7 | 8 |
| Λ - $[\text{Ru}(\text{phen})_2(\text{phi})]^{2+}$ | 1.26 | 6.8 | 8 |

a) K_B =intrinsic binding constant, b) n =average numbers of base pairs of DNA occupied by one chiral complex, c) R =red shift of the absorption peak at 535 nm (for both complexes).

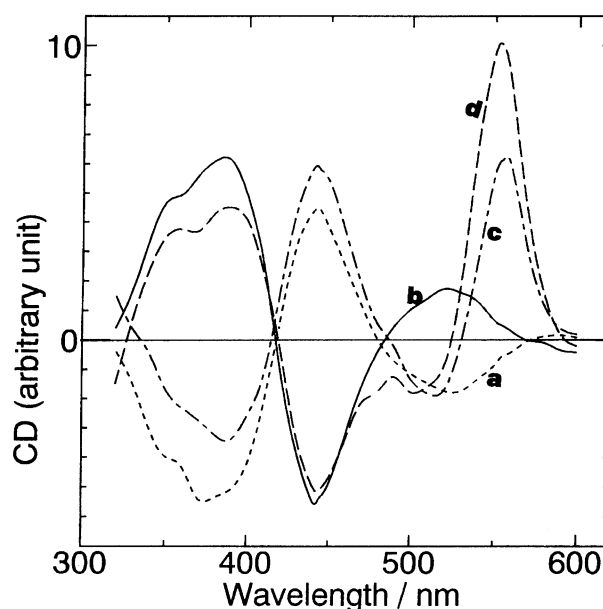


Fig. 5. CD spectra of (a) free Λ - $[\text{Ru}(\text{phen})_2(\text{phi})]^{2+}$ (1.83×10^{-5} M); (b) free Δ - $[\text{Ru}(\text{phen})_2(\text{phi})]^{2+}$ (1.85×10^{-5} M); (c) Λ - $[\text{Ru}(\text{phen})_2(\text{phi})]^{2+}$ (1.83×10^{-5} M) and calf thymus DNA (1.38×10^{-4} M); (d) Δ - $[\text{Ru}(\text{phen})_2(\text{phi})]^{2+}$ (1.85×10^{-5} M) and calf thymus DNA (1.47×10^{-4} M).

trum, a free Δ -isomer has a positive band around 520–550 nm. On binding to DNA, the peak position of the band shifts towards the longer wavelength by about 30 nm with a concomitant increase of the amplitude from $\Delta\varepsilon = +1.7$ to $+10$. For the Λ -isomer, the negative band around 520–550 nm reverses the sign to positive on binding to DNA. The peak position shifts towards a longer wavelength by 30 nm and $\Delta\varepsilon$ changes from -1.8 to $+6.2$. As a result, the absorption bands around 520–550 nm for both enantiomers have the same positive sign on a DNA strand. The behaviors may be attributed to the induction of positive CD due to the asymmetric environment of the right-handed helicity of DNA. The results suggest that the phi ligands of both enantiomers penetrate deeply into the DNA double helices. The CD results for the systems of $[\text{Ru}(\text{pby})_2(\text{phi})]^{2+}$ and calf thymus DNA are shown in Fig. 6. The similar inversion of the sign of the band at 520–550 nm is observed

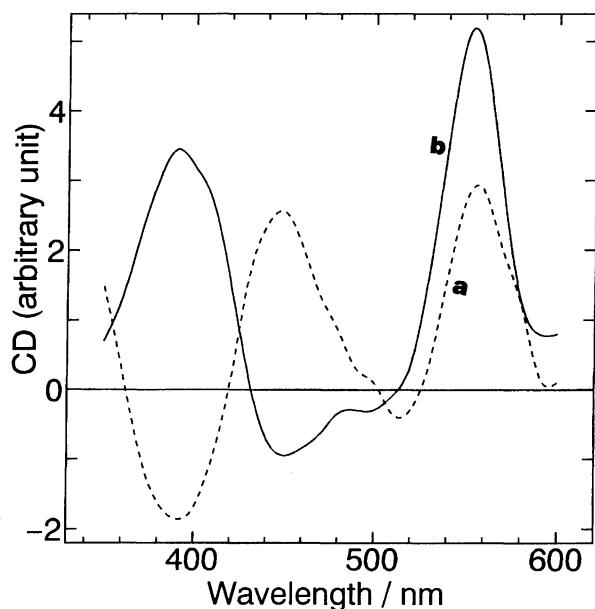


Fig. 6. CD spectra of (a) Λ -[Ru(bpy)₂(ϕ)]²⁺ (1.56×10^{-5} M) and calf thymus DNA (1.04×10^{-4} M); (b) Δ -[Ru(bpy)₂(ϕ)]²⁺ (1.66×10^{-5} M) and calf thymus DNA (1.42×10^{-4} M).

for Λ -[Ru(bpy)₂(ϕ)]²⁺, indicating that the ϕ ligand of the bound complex penetrates the DNA helices. The absorbance band in the region of 350–500 nm shows little change on binding to DNA.

LD Measurements. The orientation of an enantiomer bound to DNA is studied by an electric linear dichroism (LD) technique. The electric dichroism is measured by applying an electric field pulse of 0.54 – $5.46 \text{ kV cm}^{-1} \times 400 \mu\text{s}$ on a solution of chiral complex-DNA. The induced change of absorbance obeys the following equation of orientational dichroism;²¹⁾

$$\Delta A/A = (\rho/6)(1 + 2 \cos 2\theta), \quad (3)$$

in which $\Delta A/A$ and θ denote the relative absorbance change and the angle between the electric field and the polarization of monitoring light, respectively. ρ is the reduced linear dichroism defined by

$$\rho = (\varepsilon_{\parallel} + \varepsilon_{\perp})/\varepsilon, \quad (4)$$

in which ε , ε_{\perp} , and ε_{\parallel} are the extinction coefficient for nonpolarized, perpendicularly polarized, and paralleled polarized lights, respectively.

Figures 7 and 8 show the results for the systems of bound [Ru(bpy)₂(ϕ)]²⁺ and [Ru(phen)₂(ϕ)]²⁺ enantiomers, respectively, in which ΔA at 5.46 kV cm^{-1} is plotted as a function of wavelength from 380 to 600 nm covering the MLCT absorptions to phen or bpy and ϕ ligands. The MLCT absorption band at 520–550 nm shows largely negative dichroism. A Λ -isomer has a little more negative amplitude than a Δ -isomer. The dichroism in the MLCT absorption band at 400–480 nm shows a smaller amplitude. A Λ -isomer has a pos-

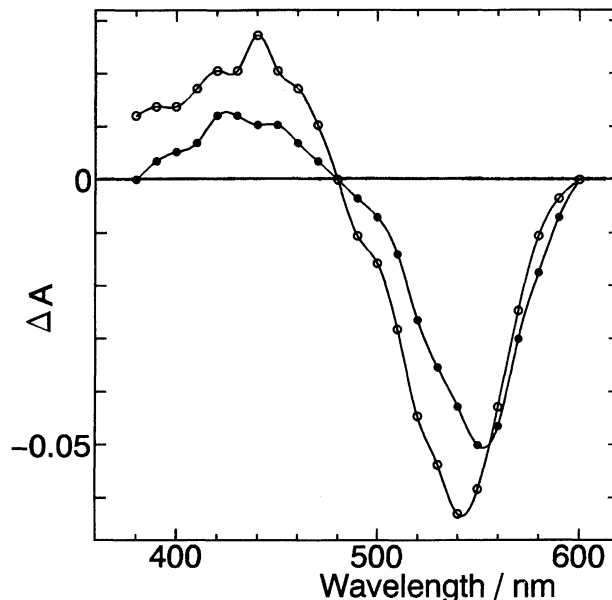


Fig. 7. Wavelength dependence of ΔA at $\theta=0^\circ$ for (●) Δ -[Ru(phen)₂(ϕ)]²⁺ (1.85×10^{-5} M) and calf thymus DNA (1.47×10^{-4} M); (○) Λ -[Ru(phen)₂(ϕ)]²⁺ (1.83×10^{-5} M) and calf thymus DNA (1.38×10^{-4} M).

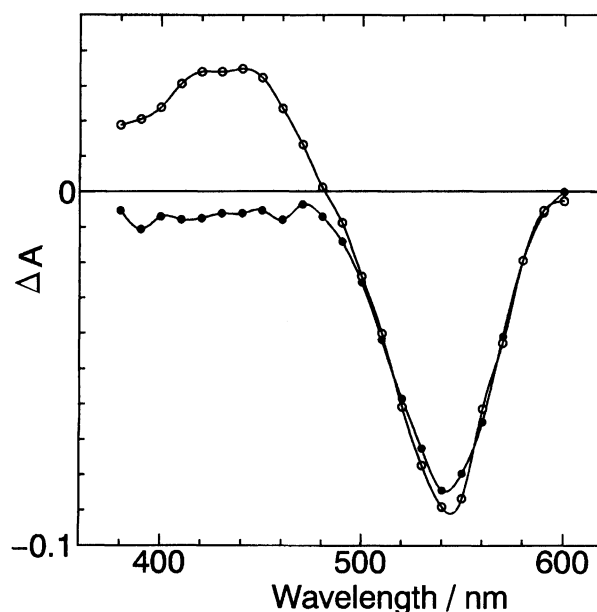


Fig. 8. Wavelength dependence of ΔA at $\theta=0^\circ$ for (●) Δ -[Ru(bpy)₂(ϕ)]²⁺ (1.66×10^{-5} M) and calf thymus DNA (1.42×10^{-4} M); (○) Λ -[Ru(bpy)₂(ϕ)]²⁺ (1.55×10^{-5} M) and calf thymus DNA (1.04×10^{-4} M).

itive dichroism, while a Δ -isomer has nearly zero or negative dichroism.

Reduced linear dichroism (ρ) in Eq. 3 is a function of an angle between the transition moment (μ) of electronic absorption and the electric field direction. The MLCT band due to the ϕ ligand has the μ directed from a Ru(II) atom to the ligand along the short axis of it. Based on this, ρ is expressed by the following

Table 2. The Reduced Linear Dichroism at Complete Orientation (ρ/Φ) and Orientational Angles, Ψ_1 and Ψ_2 (in Degrees) for Chiral Ruthenium Complexes Bound to Calf Thymus DNA (See Text as for the Definition of Ψ_1 and Ψ_2)

| Enantiomers | ρ/Φ | Ψ_1 | ρ/Φ | Ψ_2 | ρ/Φ | Ψ_2 |
|--|-------------|----------|-------------|----------|-------------|----------|
| Δ -[Ru(bpy) ₂ (phi)] ²⁺ | -0.93 | 77 | -0.29 | 52 | -0.15 | 56 |
| Λ -[Ru(bpy) ₂ (phi)] ²⁺ | -0.51 | 70 | 0.27 | 69 | 0.1 | 64 |
| Δ -[Ru(phen) ₂ (phi)] ²⁺ | -0.70 | 72 | 0.28 | 70 | 0.37 | 73 |
| Λ -[Ru(phen) ₂ (phi)] ²⁺ | -0.87 | 76 | 0.45 | 76 | 0.32 | 71 |

equation:²¹⁾

$$\rho = (3/4)(1 + 3 \cos 2\Psi_1)\Phi(E), \quad (5)$$

where $\Phi(E)$ is the orientation function representing the degree of the fraction of DNA polymer aligned in the electric field (E) direction and Ψ_1 is the angle between the C_2 axis, which is parallel to the transition moment of MLCT band (phi ligand), and the helical axis of DNA.

$\Phi(E)$ is calculated from the dependence of the dichroism amplitude on the electric field strength. $\Phi(E)$ is assumed to obey the following equation:²²⁾

$$\Psi(E) = 1 - 3(\coth X - 1/X)/X, \quad (6a)$$

$$X = \mu E/kT, \quad (6b)$$

in which μ is the dipole moment of DNA and k , Boltzmann's constant. By comparing the dependence of ρ on E for the range of $E=0.54$ – 5.46 kV cm^{-1} with Eq. 6a, we choose as 5.79×10^{-4} the best value of μ/kT as shown in Fig. 9. From this value, $\Phi(E)$ is calculated to be 0.35 at $E=5.46$ kV cm^{-1} .

The MLCT band due to the phen or bpy ligands is composed of two independent μ 's: one (μ_1) is directed along the short axis of one phen or bpy ligand and the other (μ_2) perpendicular to μ_1 .¹⁸⁾ Both μ_1 and μ_2 are on the plane perpendicular to the pseudo C_3 axis of a complex. Supposing that these transition moments take the same probability in any direction on that plane, ρ is given by the following equation:²³⁾

$$\rho = -(3/8)(1 + 3 \cos 2\Psi_2)\Phi(E), \quad (7)$$

where Ψ_2 denotes the angle between the C_3 axis of a complex and the electric field direction.

Table 2 shows the results of the electric dichroism in which ρ/Φ , Ψ_1 , and Ψ_2 are given for the enantiomers of [Ru(phen)₂(phi)]²⁺ and [Ru(bpy)₂(phi)]²⁺ bound to calf thymus DNA. ρ/Φ is the reduced linear dichroism for complete orientation at wavelengths (nm) of 540 (phi), 450 and 420 (two phen's), and 450 and 420 (two bpy's). Ψ_1 and Ψ_2 are the orientational angles in degrees.

Discussion

In this study we have tried to elucidate the binding structure of chiral metal complexes with calf thymus

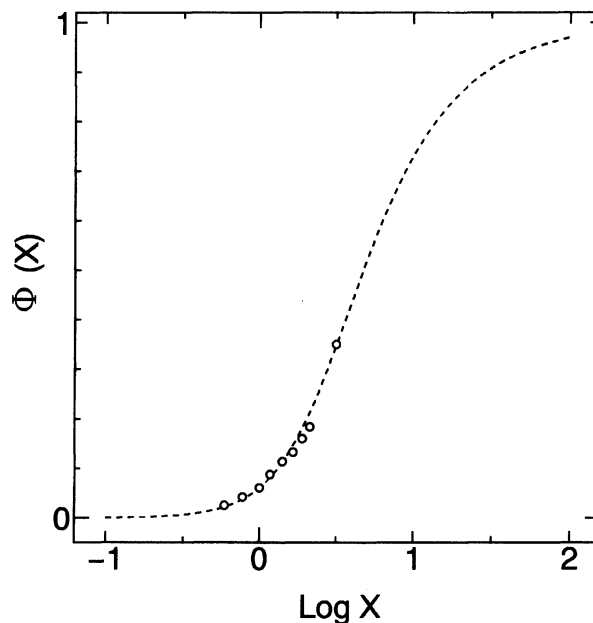


Fig. 9. Plot of $\Phi(E)$ vs. $\log X$ for the system of Δ -[Ru(bpy)₂(phi)]²⁺ and calf thymus DNA. (---) represents the theoretical curve calculated from Eq. 6a and (O), the experimental values obtained from $E=0.54$ – 5.46 kV cm^{-1} . Here X represents $\mu E/KT$ in which μ is the permanent dipole moment of DNA, K , the Boltzmann constant and T , absolute temperature.

DNA. Measurements have been done to obtain binding constants and CD and LD spectra.

The binding constant (K_B) was measured for the binding of enantiomeric [Ru(bpy)₂(phi)]²⁺ and [Ru(phen)₂(phi)]²⁺ with calf thymus DNA. The enantiomers are bound to the DNA with K_B larger than 10^{-4} M^{-1} (Table 1). These values are more than 10 times larger than those obtained for [Ru(bpy)₃]²⁺ and [Ru(phen)₃]²⁺.⁷⁾ Thus the presence of the phi ligand increases affinity towards the DNA.

CD spectra give us information on how the helicity of the DNA chain influences the electronic transitions of a bound complex. A large induction effect by the chain helicity was observed on the spectrum of a bound complex in the MLCT region from a Ru(II) atom to a phi ligand. In the cases of both Δ - and Λ -enantiomers, the binding with the DNA shifts the CD band towards

the positive direction. For the Λ -enantiomer, the effect is so prominent that the sign of the band is reversed from the negative sign to the positive one. Based on the results, we conclude that the phi ligands of both complexes are very close to the helical backbone.

LD spectra identify the orientation of the transition moment of a bound complex with respect to the helical axis. LD measurements assist the above conclusions by showing that the phi ligands orient roughly perpendicular to the helical axis (Table 2). When the complexes intercalate their phi ligands between the basepairs, the ligands eventually take the direction perpendicular to the helical axis.

The idea of intercalation of one of the ligands of a bound complex was first proposed by Barton in the case of $[\text{Zn}(\text{phen})_3]^{2+}$.³⁾ By applying the electric dichroism measurements on $[\text{Ru}(\text{phen})_3]^{2+}$ and $[\text{Ru}(\text{bpy})_3]^{2+}$, we previously showed that the Δ -enantiomer is intercalated between the basepairs, while the Λ -enantiomer is bound in the outer sphere of DNA.¹⁰⁾ Due to the highly symmetrical properties of the Ru(II) complex, however, the transition moments in the MLCT band consist of two composites which are perpendicular. These situations caused some ambiguity in interpreting the LD results.²⁴⁾ In contrast to $[\text{Ru}(\text{phen})_3]^{2+}$ and $[\text{Ru}(\text{bpy})_3]^{2+}$, there is no such ambiguity in these cases. The orientation of the phi ligand is identified uniquely because the MLCT band from the Ru(II) atom to the phi ligand has a characteristic absorption band at the longer wavelength. As a result, both enantiomers are concluded to intercalate their phi ligands between the base pairs.

As for the orientation of two ancillary (bpy or phen) ligands, the LD spectra show definite differences between the Δ - and Λ -isomers for both $[\text{Ru}(\text{bpy})_2(\text{phi})]^{2+}$ and $[\text{Ru}(\text{phen})_2(\text{phi})]^{2+}$ complexes. For the Λ -isomers (Figs. 7 and 8), the dichroism amplitude at $\theta=0^\circ$, $\Delta A(\theta)$, is positive in the range of 400–450 nm, while $\Delta A(\theta)$ for Δ -isomer is nearly zero or negative in this wavelength region. The absorption bands in this region contain two transitions related to the MLCT from the Ru(II) ion to two bpy or phen ligands.¹⁰⁾ As a result, the plane containing these two transition moments is concluded to be oriented in the different directions between the Δ - and Λ -isomers, although the differences in angles are very small. These differences may arise from the steric hindrance from the helical periphery of the

DNA.

References

- 1) H. Y. Mei and J. K. Barton, *Proc. Natl. Acad. Sci. U.S.A.*, **85**, 1339 (1988).
- 2) B. Norden and F. Tjernereld, *FEBS Lett.*, **67**, 368 (1976).
- 3) J. K. Barton, J. J. Dannenberg, and A. L. Raphael, *J. Am. Chem. Soc.*, **104**, 4967 (1982).
- 4) A. Yamagishi, *J. Chem. Soc., Chem. Commun.*, **1983**, 572.
- 5) J. K. Barton, A. T. Danishefsky, and J. M. Goldberg, *J. Am. Chem. Soc.*, **106**, 2172 (1984).
- 6) J. K. Barton, J. M. Goldberg, C. V. Kumar, and N. J. Turro, *J. Am. Chem. Soc.*, **108**, 2081 (1986).
- 7) A. M. Pyle, J. P. Rehmann, R. Meshoyrer, C. V. Kumar, N. J. Turro, and J. K. Barton, *J. Am. Chem. Soc.*, **111**, 3051 (1989).
- 8) J. K. Barton, *J. Biomol. Struct. Dyn.*, **1**, 621 (1983).
- 9) J. K. Barton, *Science*, **233**, 727 (1986).
- 10) A. Yamagishi, *J. Phys. Chem.*, **88**, 5709 (1984).
- 11) Kyaw Naing, M. Takahashi, M. Taniguchi, and A. Yamagishi, *J. Chem. Soc., Chem. Commun.*, **1993**, 402.
- 12) S. S. David and J. K. Barton, *J. Am. Chem. Soc.*, **115**, 2984 (1993).
- 13) C. Hiort, P. Lincoln, and B. Norden, *J. Am. Chem. Soc.*, **115**, 3448 (1993).
- 14) P. Belser, A. Von Zelewsky, and M. Zehnder, *Inorg. Chem.*, **20**, 3098 (1981).
- 15) B. Bosnich and F. P. Dwyer, *Aust. J. Chem.*, **19**, 2229 (1966).
- 16) G. Felsenfeld and S. Z. Hirschman, *J. Mol. Biol.*, **13**, 407 (1965).
- 17) M. Taniguchi, A. Yamagishi, and T. Iwamoto, *Inorg. Chem.*, **30**, 2462 (1991).
- 18) B. Bosnich, *Inorg. Chem.*, **7**, 178 (1968).
- 19) V. A. Bloomfield, D. M. Crothers, and I. Tinoco, Jr., "Physical Chemistry of Nucleic Acids," Harper and Row, New York (1974), p. 432.
- 20) A. Wolfe, G. H. Shimer, and T. Meehan, *Biochemistry*, **26**, 6392 (1987).
- 21) M. Dourlent, J. F. Horgel, and C. Helene, *J. Am. Chem. Soc.*, **96**, 3398 (1974).
- 22) Da-wen Ding, R. Rill, and K. E. Van Holde, *Biopolymers*, **11**, 2109 (1972).
- 23) A. Yamagishi, *J. Phys. Chem.*, **86**, 2472 (1982).
- 24) C. Hiort, B. Norden, and A. Rodger, *J. Am. Chem. Soc.*, **112**, 1971 (1990).